Catalysis Letters Vol. 106, Nos. 1–2, January 2006 (© 2006)
DOI: 10.1007/s10562-005-9188-1

Kinetic study of the steam reforming of isobutane using a $Pt–CeO_2–Gd_2O_3$ Catalyst

Chethan K. Acharya[a], Alan M. Lane[a,*], and Theodore R. Krause[b]

[a]*Department of Chemical Engineering, The University of Alabama, 870203, Tuscaloosa, AL 35487, USA*
[b]*Chemical Engineering Division, Argonne National Laboratory, 9700 South Cass Avenue, Bldg. 205, Argonne, IL 60439, USA*

Received 29 May 2005; accepted 21 September 2005

Steam reforming of isobutane on a 0.5% $Pt–Ce_{0.8}Gd_{0.2}O_{1.9}$ catalyst was carried out from 300 to 700 °C under integral conditions with a gas hourly space velocity (GHSV) of 12,000 h^{-1}. The major products were H_2, CO_2, CO and CH_4. The other products produced were ethane, ethylene, propane and propylene with a total molar composition of less than 1.5%. A complete conversion of isobutane was achieved at 700 °C, Kinetic data was obtained by changing the partial pressure of the reactants and the temperature under differential conditions with a GHSV of 55,400 h^{-1}. This was done after observing stable isobutane steam reforming for 160 h and under conditions where the mass transfer limitations were insignificant. An empirical Langmuir–Hinshelwood type model that best fit the kinetic data available was developed.

KEY WORDS: steam reforming; isobutane; platinum/ceria-gadolinia; kinetics.

1. Introduction

Hydrogen for use in fuel cell-powered propulsion systems for automotive applications can be produced on-board by reforming a hydrocarbon by one of the three processes: (a) partial oxidation; (b) steam reforming; and (c) autothermal reforming. Autothermal reforming is a combination of exothermic partial oxidation and endothermic steam reforming resulting in thermoneutral conditions. Its advantages in an on-board fuel processor have been outlined by Flynn *et al.* [1], which include: (a) easy thermal integration; (b) a light and compact fuel processor; and (c) fast start up and transient response. The catalyst controls the reaction pathways and thereby determines the relative extent of partial oxidation and steam reforming.

Hydrocarbons from C_1 to C_{14} have been used as a fuel for reforming. Christiansen [2] first investigated steam reforming of methanol over reduced copper in 1921. Research has continued on methanol steam reforming over different catalysts such as:Cu–Mn, Cu–Cr–Zn, Cu–Ni–Fe, Cu–Cr, Cu–Co, Fe–Cr–Ni and $Cu–ZnO–Al_2O_3$ [3–6]. Natural gas, methane, ethanol, propane and butane can also be used as fuels for hydrogen production [7–15]. To facilitate the transition between the internal combustion engine and fuel cell vehicles, hydrocarbons like gasoline and diesel have to be used to produce hydrogen.

Nickel based catalysts are very good for steam reforming C_4 and higher hydrocarbons [16]. But, they deactivate quickly due to coke formation [17–21] and also must be reduced before the reaction to optimize the catalytic activity, which is difficult for automotive applications [1].

The noble metal (Pt, Pd, Rh and Ru) based catalysts are drawing attention for autothermal and steam reforming of hydrocarbons. The main advantages of using them for on-board reforming processes are: (a) they are as active or more active than nickel reforming catalysts [16, 22]; (b) they can suppress coke formation [23, 24]; and (c) no pretreatment is required before the reaction because they promote reforming under both oxidizing and reducing conditions [1]. The reforming ability of the noble metal based catalysts depends on the support used: (a) non-reducible supports (Al_2O_3, ZrO_2); and (b) reducible or redox supports (CeO_2). Gorte *et al.* [23, 24] carried out steam reforming of Various hydrocarbons like *n*-butane, *n*-hexane, *n*-octane, benzene and toluene on Pd/ceria and Pd/Al_2O_3 catalysts between 620 and 700 K. They found the Pd/ceria catalyst exhibits a higher rate and selectivity for most reactions compared to the Pd/Al_2O_3 catalyst. They proposed a dual-function mechanism in which CeO_2 transfers oxygen to the metal and is in turn reduced to Ce_2O_3. The reduced ceria is then re-oxidized by water to CeO_2, thus acting as an oxygen storage device, supplying oxygen to hydrocarbons adsorbed on the supported metal for oxidation.

The oxygen mobility in the ceria support to the active metal for hydrocarbon reforming can be accelerated by creating vacancies in the ceria lattice [25], which can be achieved by doping ceria with a trivalent cationic oxide (M_2O_3). It creates extrinsic vacancies in the ceria lattice based on the principle of charge compensation [26].

* To whom correspondence should be addressed.
E-mail: ALANE@coe.eng.ua.edu

Gorte *et al.* [27, 28] have shown that dopants like oxides of Fe, Tb, Gd, Y, Sn, Sm, Pr, Eu, Bi, Cr, V, Pb and Mo in ceria have different influence on different reactions and the appropriateness of a dopant for a particular reaction should be tested without generalizing. Studies at Argonne National Laboratory (ANL) have shown that Group VIII metals such as platinum, dispersed on oxide-ion conducting supports such as gadoliniadoped ceria are active catalysts for reforming a wide range of hydrocarbons including natural gas, gasoline, and diesel [29, 30]. The isobutane steam reforming kinetics on a Pt/ceria/gadolinia catalyst will be discussed in this paper without making a comparative study with other catalysts on the activity.

The motivation for carrying out steam reforming is that, in autothermal reforming, more than 70% of the hydrogen on a dry basis is produced during the steam reforming stage [31] and it is a slow reaction. It therefore becomes necessary to study the kinetics of steam reforming as a step towards understanding autothermal reforming in which, partial oxidation occurs first followed by steam reforming. When hydrocarbons like gasoline are reformed, they quickly break down to lower hydrocarbons like C_4 during the partial oxidation stage and subsequently undergo steam reforming. Isobutane was hence used as a model fuel for carrying out steam reforming.

2. Experimental

The schematic diagram of the steam reforming reactor is shown in figure 1. Isobutane of 99.9% purity and ultra high purity nitrogen (99.99%) supplied by Air Gas were mixed with deionized water fed by a syringe pump (KD Scientific, model 100). The flow rate of the gases was controlled by mass flow controllers (UNIT, 8100 series). The nitrogen was used as an internal standard gas to account for the volume expansion factor. The mixture entered a U-tube filled with SiC (Pfaltz & Bauer, Inc.) to enhance mixing and at the same time was heated to 160 °C by a heating tape wound around the U-tube to convert water to steam. The temperature of the vaporizer was monitored by a temperature recorder. A pressure gauge in the gas inlet line monitored the pressure in the system. From the U-tube, the gas mixture entered a 0.35 inch quartz tube reactor containing a quartz wool bed that supported the catalyst. A furnace encompassing the quartz tube supplied the heat for the reaction. The temperature of the furnace was set by a temperature controller, which sensed the temperature from a thermocouple at the top of the catalyst bed. Another thermocouple monitored the bottom temperature of the catalyst bed. The products flowed to a condenser maintained at room temperature and a drierite bed (anhydrous calcium sulfate), where the water was removed. After removing most of the condensable water, a sample was taken in a six-way valve and injected into an HP 5890 Gas Chromatograph (GC) with a Haysep DB packed column and a TCD detector. The GC was connected to an SRI PeakSimple data acquisition system.

The catalyst formulation was developed at Argonne National Laboratory [29]. The catalyst denoted as 0.5% Pt–CGO-20, consisted of Pt (0.5 wt%) supported on mixed oxide consisting of 80% ceria and 20% gadolinia ($Ce_{0.8}Gd_{0.2}O_{1.9}$). The BET surface area of the catalyst was 36.5 m^2/g.

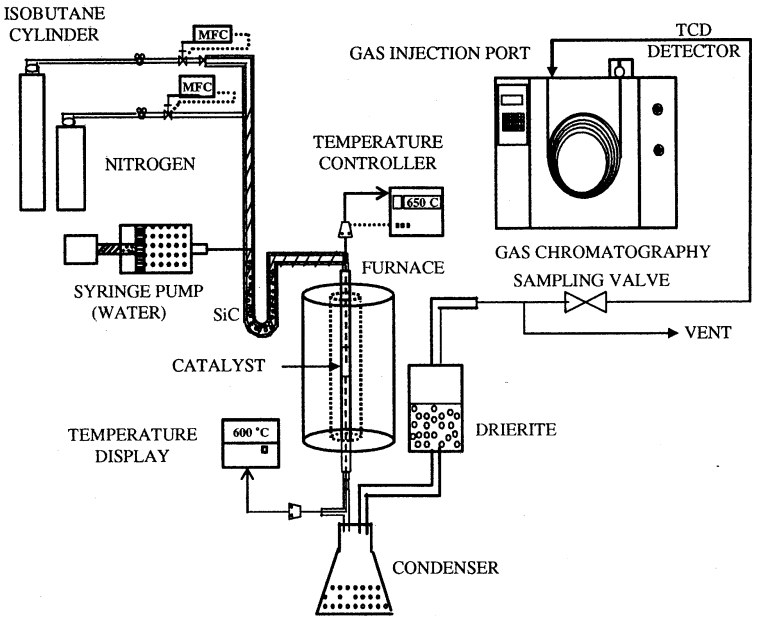

Figure 1. Schematic diagram of the steam reforming reactor.

The reactions were carried out under integral and differential conditions. The Integral conditions were 300–700 °C, 1.09 atm total pressure, 12,000 h^{-1} GHSV and 107 ml/min (STP) total flow rate. The catalyst weight used was 0.5 g. Under differential conditions, 0.1 g of the catalyst mixed with 0.1 g of SiC was subjected to steam reforming from 480–550 °C, 1.09 atm total pressure, 55,400 h^{-1} GHSV and 146 ml/min (STP) total flow rate. Even though the partial pressure of the reactants was changed, the total pressure was maintained at 1.09 atm by adjusting the partial pressure of nitrogen. The water to carbon molar ratio was 2 (stoichiometric ratio) in most of the reactions except during the kinetic study. Under differential conditions, the conversion of isobutane was maintained below 10%. The reaction product was sampled after 1 h of reaction at a particular condition until reproducible results were obtained. In all experiments the catalyst was not pretreated.

3. Results and discussion

3.1. Integral reaction

The reaction yield (mol/mol of isobutane in the feed) of products and isobutane conversion at different temperatures under integral conditions is shown in figure 2. The reaction was initiated at 300 °C and reached completion at 700 °C. The yield of H_2 and CO_2 increased with temperature. Above 650 °C, the slope of H_2 and CO_2 curves decreased and the CO yield increased significantly with temperature. This was due to the reverse water gas shift reaction ($H_2 + CO_2 \leftrightarrow CO + H_2O$), which can be corroborated from the fact that the Pt/CeO_2 catalysts are very active for water gas shift reactions [16, 32]. Methane was detected at 400 °C and the yield increased with temperature. The other minor byproducts with a total molar composition of less than 1.5% were ethylene, ethane, propylene and propane (not shown in the figure). The carbon balance between the feed and the product was reasonable with a maximum deviation of 11%.

The mol% of H_2, CO, CO_2 and CH_4 at 700 °C was 63, 15, 15 and 4% respectively, which was comparable to the results reported in the literature when noble metal/CeO_2 (with or without a dopant) catalysts were used for hydrocarbon steam reforming. Suzuki *et al.* [33] performed steam reforming of kerosene on a Ru/CeO_2–Al_2O_3 catalyst and observed a similar product distribution at 800 °C. Breen *et al.* [34] carried out ethanol steam reforming on a $Pt/CeO_2/ZrO_2$ from 350 to 700 °C. At 700 °C the product distribution was comparable to our result.

The reaction yield was compared with the equilibrium yield of the reforming reaction. Kinetic factors also influence the product distribution but equilibrium yield provides a useful limiting case, especially at high temperature. It was obtained using a chemical engineering process simulation software package (Chemstations ChemCAD 5.4), based on Gibbs free-energy minimization. In the simulation the H_2O/C ratio was 2 and all the possible products namely H_2, CO, CO_2, CH_4, C_2H_4, C_2H_6, C_3H_6, C_3H_8 and C were specified in the reactor outlet stream. The simulation calculated the equilibrium molar composition of the products as a function of temperature from which the yield was calculated. Figure 3 shows the equilibrium yield of the major products from 300 to 700 °C. The H_2 and CO yield increased with temperature. The CO yield increased significantly after 500 °C. The CO_2 yield increased from 300 to 550 °C and then decreased. The calculated equilibrium yields of H_2, CO_2 and CO were similar to the experimental yields especially at higher temperatures. However, the calculated methane yield was

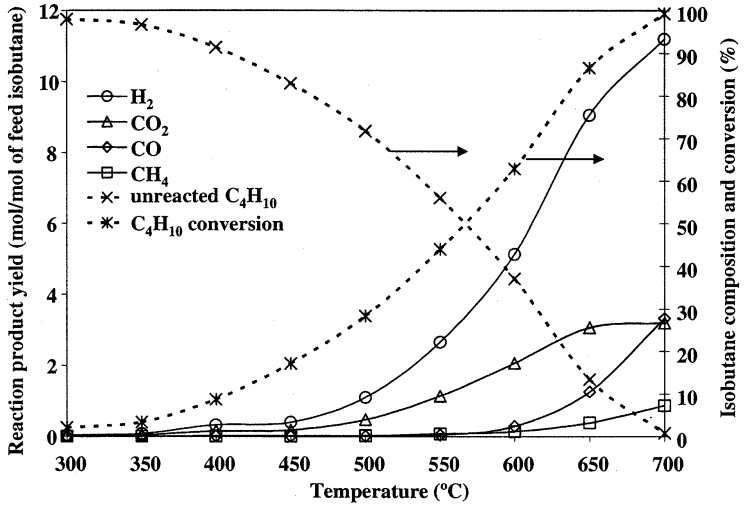

Figure 2. Reaction yield of the products of isobutane steam reforming and conversion at different temperatures on the 0.5% Pt-CGO-20 catalyst.

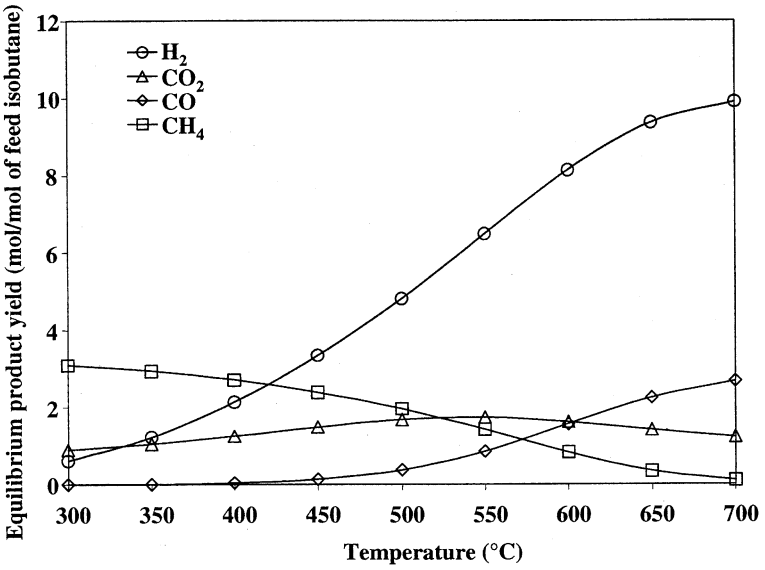

Figure 3. Equilibrium yield of the products of isobutane steam reforming at different temperatures.

highest at 300 °C and decreased with temperature. The methane may have been produced from syngas that was more plentiful at higher conversion.

3.2. Stability test

To study the kinetics of isobutane steam reforming on the 0.5% Pt–CGO-20 catalyst, the reaction was carried out under gradientless conditions. Two major factors were considered before the kinetic data for steam reforming was obtained: (a) the stability of the catalyst; and (b) the external and internal mass transfer limitations. Experiments were carried out to find the appropriate conditions for these factors to be insignificant.

The stability of the 0.5% Pt–COO-20 catalyst tested under differential conditions is shown figure 4. The figure shows the rate of isobutane consumption as a function of time at 550 °C for 160 h. The rate was calculated using the formula

$$r_{ib} = F_{ib}{}^{*} X_{ib}/W \quad (1)$$

where r_{ib} is the rate of isobutane consumption; F_{ib} is the molar flow rate of isobutane; X is the conversion of isobutane; and W is the weight of the catalyst. The catalyst showed a stable reforming rate of 0.42 with a ± 0.05 millimol/s g standard deviation.

3.3. Mass transfer limitations

To examine the possibility of external mass transfer limitations, differential steam reforming was carried out under two different reaction conditions with the same

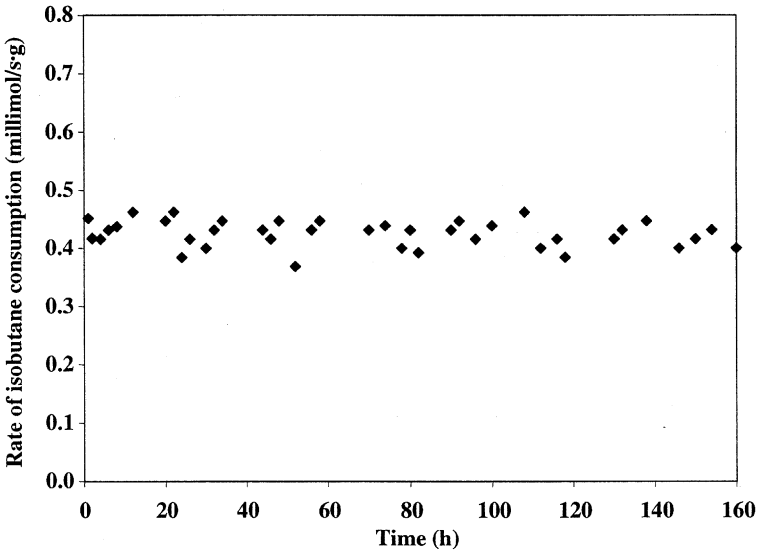

Figure 4. Activity of the 0.5% Pt-CGO-20 catalyst for 160 h at 550 °C under differential conditions.

catalyst size (0.9–0.3 mm). Under the first set of conditions, the reaction parameters were the same as that of the stability test. Under the second set of conditions, the total flow rate was doubled to 292 ml/min by doubling the molar flow rate of all the inlet gases. This resulted in doubling the linear velocity of the feed along the length of the reactor. The amount of the catalyst used was also doubled to maintain the same space velocity. The rate must remain the same if the reaction is not mass transfer limited. Table 1 shows that the rate of isobutane consumption at the two different inlet flow conditions were the same, within experimental error. Under these flow conditions, external mass transfer was negligible.

To examine the possibility of internal mass transfer limitations, differential steam reforming was carried out on a 0.13–0.10 mm size catalyst with the reaction parameters the same as that of the first case in the external mass transfer limitation test. The rate was compared with that of the 0.9–0.3 min size catalyst. The comparison is shown in table 1. The rates were the same, within experimental error. In addition, the Weisz–Prater criterion [35], used to determine if the internal diffusion limits the reaction, was estimated to be 0.03 with the 0.9–0.3 mm catalyst, which was $< < 1$, eliminating the possibility of the internal diffusion limitations. Based on the criterion the internal diffusion limits the reaction when a 4 mm or higher size catalyst is used.

3.4. Kinetic data at different steam partial pressures

Kinetic data was obtained by changing the partial pressure of the reactants at a constant total pressure of 1.09 atm, GHSV of 55,400 h^{-1} and a total flow rate of 146 ml/min at different temperatures. About 0.1 g of the 0.9–0.3 mm 0.5% Pt–CGO-20 catalyst mixed with a 0.1 g of SiC was used. Under these flow conditions and size of the catalyst, mass transfer limitations were insignificant as shown earlier.

The partial pressure of steam was changed at a constant isobutane partial pressure of 0.09 atm. The H_2O/C ratio was varied from 0.9 to 2.7 at four different temperatures of 480, 500, 530 and 550 °C. The rate of isobutane consumption as a function of steam partial pressure is shown in figure 5. The rate had a non-monotonic dependence on the steam partial pressure at all the temperatures. The drop in the reaction rate at high steam partial pressures could be due to the excess water molecules blocking the active sites, making them unavailable for the isobutane to adsorb and take part in the reaction.

3.5. Kinetic data at different isobutane partial pressures

Kinetic data was also obtained by changing the isobutane partial pressure at a constant steam partial pressure of 0.6 atm. The H_2O/C ratio was varied from 0.7 to 3.2 at four different temperatures of 480, 500, 530 and 550 °C. The rate as a function of the isobutane partial pressure is shown in figure 6. The rate increased and plateaued with the partial pressure of isobutane at all the temperatures. The change in the slope of the line occurred at a H_2O to C ratio of 2, which could be due to the saturation of active sites with isobutane.

An empirical model, of a Langmuir–Hinshelwood form, was developed to best fit the kinetic data obtained from the experiments

$$r_{ib} = \frac{\left(k_o e^{-(E_a/RT)} K_1 K_2 P_{ib} P_w\right)}{\left(1 + K_1 P_{ib} + K_2 P_w^2\right)} \quad (2)$$

k_o (frequency factor) = 32 mol/s g cat atm^2, K_1 (equilibrium constant) = 2811 atm^{-1}, K_2 (equilibrium constant) = 406 atm^{-1}, E_a (activation energy) = 110 kJ/mol, R (ideal gas constant) = 8.314 J/mol K

where r_{ib} is the isobutane consumption rate, T (in K) is the reaction temperature and P_{ib} and P_w (in atm) are the partial pressures of isobutane and water respectively. Figure 7 is a plot along with the correlation factor between the experimentally obtained rate data and the rate data calculated from the model. It was the best model that could be developed with the data available. No mechanistic implications can be drawn from it.

The activation energy obtained from the model was 110 kJ/mol, which was close to the activation energy obtained from the Arrhenius plot (108 ± 3 kJ/mol) as shown in figure 8, and much higher than the 64 ± 3 kJ/mol obtained by Gorte *et al.* [24] for the steam reforming of *n*-butane on a 1 wt% Pd/ceria catalyst. This could be due to the difference it the composition of the catalysts. To generate the Arrhenius plot, the rate of isobutane consumption on the catalyst was calculated at different temperatures under differential conditions. The flow conditions for the reaction were the same as that of the stability test. The samples were taken at 450, 480, 500, 530 and 550 °C after 1 h of reaction at a particular

Table 1
Rate of isobutane consumption at two different inlet gas flow rates and sizes of the 0.5% Pt-CGO-20 catalyst for mass transfer limitation tests

	External mass transfer Flow rate (ml/min)		Internal mass transfer Catalyst size (mm)	
Rate of isobutane consumption (millimol/s g)	146	292	0.9–0.3	0.13–0.10
	0.39	0.405	0.39	0.395

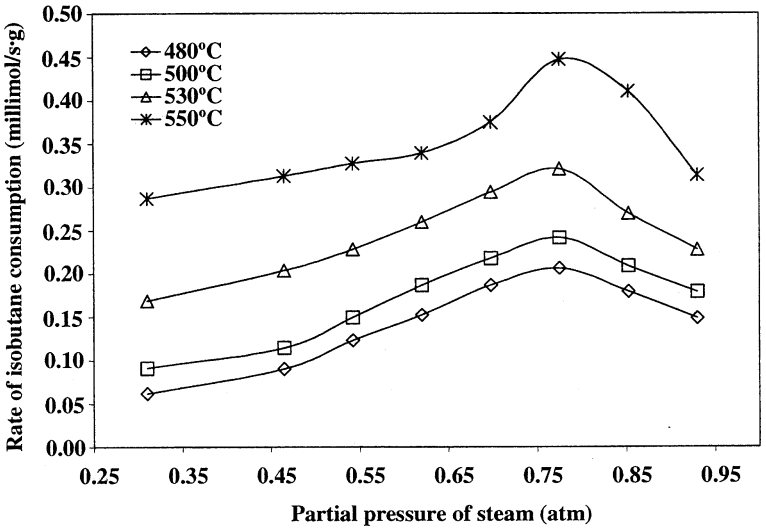

Figure 5. Effect of steam partial pressure on the reaction rate at a constant partial pressure of isobutane.

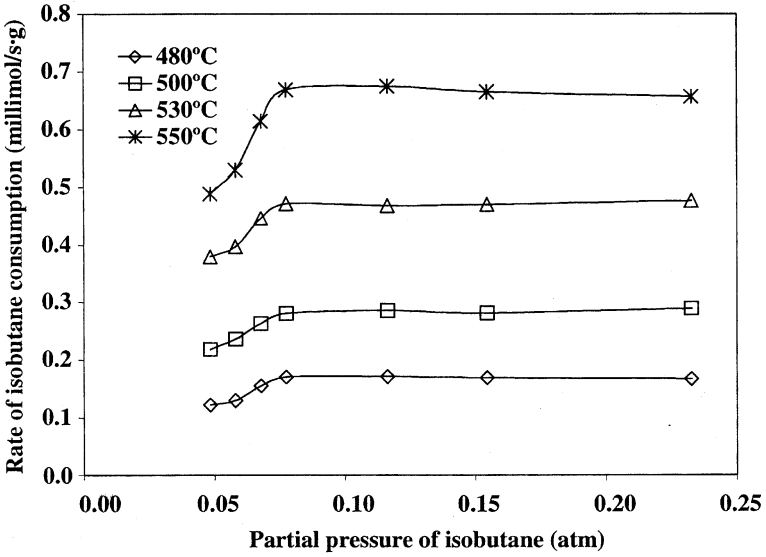

Figure 6. Effect of isobutane partial pressure on the reaction rate at a constant partial pressure of steam.

temperature until reproducible results were obtained. A linear regression lire was drawn to fit the generated data points. The slope of the line was used to calculate the activation energy of the catalyst.

4. Conclusion

The major products of the isobutane steam reforming in the presence of the 0.5% Pt–CGO-20 catalyst were H_2, CO_2, CO and CH_4. The total molar composition of the byproducts like ethane, ethylene, propane and propylene was less than 1.5%.

Under differential conditions, kinetic data was obtained using the 0.5% Pt–CGO-20 catalyst by changing the steam and isobutane partial pressures at different temperatures. At a constant isobutane partial pressure, the rate had a non-monotonic dependence on the steam partial pressure at all the temperatures. The excess water molecules could have blocked the active sites, making them unavailable for the isobutane to adsorb and take part in the reaction.

When the partial pressure of isobutane was increased at a constant steam partial pressure, the rate increased and leveled off at all the temperatures. The rate was independent of the partial pressure of isobutane above the stoichiometric proportion of the reactants, which could be due to the saturation of the active sites by isobutane.

An empirical rate model that best fit the available kinetic data was developed. The activation energy

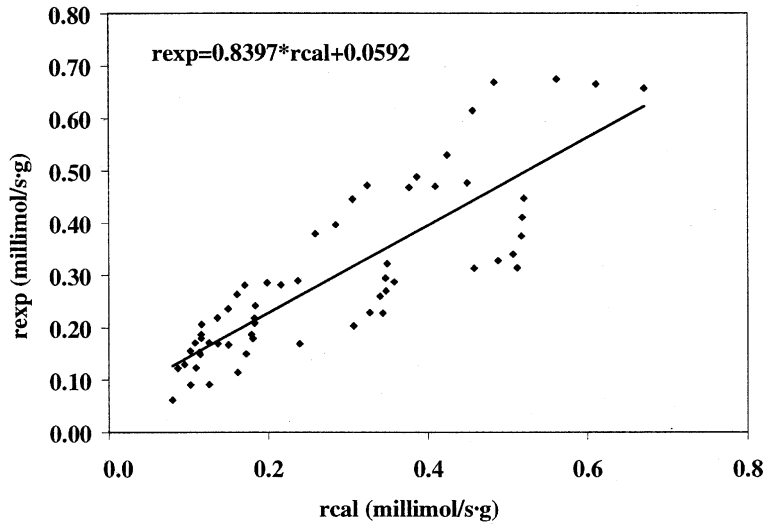

Figure 7. The line of best fit for the data points obtained experimentally and from the model.

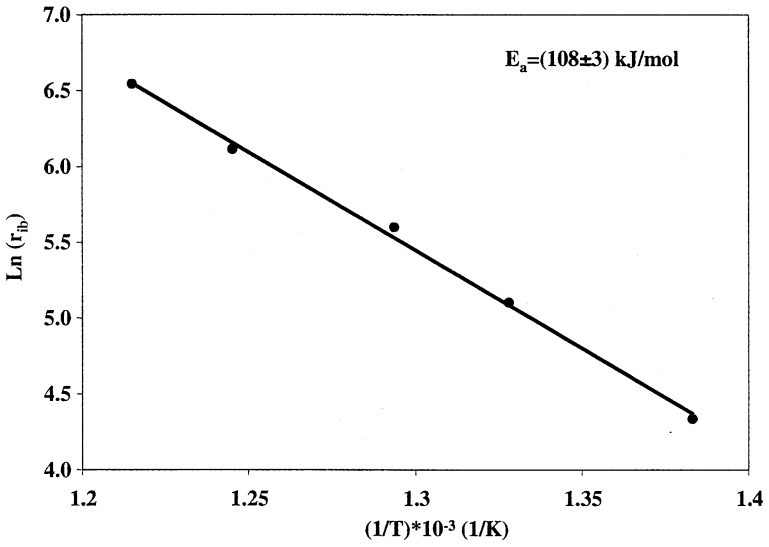

Figure 8. Arrhenius plot to calculate the activation energy of the 0.5% Pt-CGO-20 catalyst.

obtained from the model was close to the activation energy obtained from the Arrhenius plot.

Acknowledgements

The authors would like to acknowledge David Carter of the Chemical Engineering Division at Argonne National Laboratory for his assistance with preparation of the catalysts. This work was supported by the U.S. Department of Energy, Office of Energy Efficiency and Renewable Energy, Hydrogen, Fuel Cells, and Infrastructure Technologies Program. Argonne National Laboratory is operated by the University of Chicago for the Department of Energy under Contract W-31 409-ENG-38.

References

[1] T.J. Flynn, R.M. Privette, M.A. Perna, K.E. Kneidel, D.L. King and M. Cooper, SAE Technical Paper Series (1999-01-0536), International Congress and Exposition, Detroit, Michigan, Mar. 1999.
[2] J.A. Christiansen, J. Amer. Chem. Soc. 43 (1921) 1670.
[3] H. Takezawa, H. Kobayashi, A. Hirose, M. Shimokawabe and K. Takahashi, Appl. Catal. 4 (1982) 127.
[4] B.A. Peppley, J.C Amphlett, L.M. Kearns and R.F. Mann, Appl. Catal. A 179 (1999) 21.
[5] E. Santacesaria and S. Carra, Appl. Catal. 5 (1983) 345.
[6] C.J. Jiang, D.L. Trimm, M.S. Wainwright and N.W. Cant, Appl. Catal. A 93 (1993) 245.
[7] M. Prigent, Rev. Inst. Francais Petr. 52 (1997) 350.
[8] D.K. Liguras, D.I. Kondarides and X.E. Verykios, Appl. Catal. B 1344 (2003) 1.
[9] I.M. Bodrov, L.O. Apel'baum and M.I. Temkin, Kinet. Catal. 8 (1967) 821.

[10] I.M. Bodrov, L.O. Apel'baum and M.I. Temkin, Kinet. Catal. 9 (1968) 1065.
[11] N.M. Bodrov, L.O. Apel'baum and M.I. Temkin, Kinet. Catal. 5 (1964) 696.
[12] K. Hou and R. Hughes, Chem. Eng. J. 82 (2001) 311.
[13] J. Xu and G.F. Froment, AIChE J. 35 (1989) 88.
[14] A.K. Avci, D.L. Trimm, A.E. Aksoylu and Z.I. Onsan, Appl. Catal. A 258 (2004) 235.
[15] J. Mathiak, A. Heinzel, J. Roes, Th. Kalk, H. Kraus and H. Brandt, J. Power Sources 131 (2004) 112.
[16] A.F. Ghenciu, Curr. Opin. Solid State Mater. Sci. 6 (2002) 389.
[17] T. Borowiecki, Appl. Catal. 4 (1982) 223.
[18] T. Borowiecki, Appl. Catal. 31 (1987) 207.
[19] E. Tracz, R. Scholz and T. Borowiecki, Appl. Catal. 66 (1990) 133.
[20] D.J. Smith, M.R. McCartney, E. Tracz and T. Borowiecki, Ultramicroscopy 34 (1990) 54.
[21] L. Kepinski, B. Stasinska and T. Borowiecki, Carbon 38 (2000) 1845.
[22] A. Igarashi, T. Ohtaka and S. Motoki, Catal. Lett. 13 (1991) 189.
[23] X. Wang and R.J. Gorte, Catal. Lett. 73 (2001) 15.
[24] X. Wang and R.J. Gorte, Appl. Catal. A 224 (2002) 209.
[25] E.R. Cabrera, A. Atkinson and D. Chadwick, Appl. Catal. B 36 (2002) 193.
[26] B.K. Cho, J. Catal. 13 (1991) 74.
[27] S. Zhao and R.J. Gorte, Appl. Catal. A 248 (2003) 9.
[28] X. Wang and R.J. Gorte, Appl. Catal. A 247 (2003) 157.
[29] M. Krumpelt, S. Ahmed, R. Kumar and D. Rajiv, US 5,929,286, July 27, 1999.
[30] K.W. Kramarz, I.D. Bloom, R. Kumar, S. Ahmed, R. Wilkenhoener and M. Krumpelt, US 6,303,098, October 16, 2001.
[31] S. Ahmed and M. Krumpelt, Int. J. Hydrogen Energy 26 (2001) 291.
[32] G. Jacobs, S. Khalid, P.M. Patterson, D.E. Sparks and B.H. Davis, Appl. Catal. A 268 (2004) 255.
[33] T. Suzaki, H. Iwanami and T. Yoshinari, Int. J. Hydrogen Energy 25 (2000) 119.
[34] J.P. Breen, R. Burch and H.M. Coleman, Appl. Catal. B 39 (2002) 65.
[35] H.S. Fog1er, *Elements of Chemical Reaction Engineering,* 2 nd edn. (Prentice Hall, Englewood, NJ, 1992) 625.